Proceedings of the 19th International Symposium on the Packaging and Transportation of Radioactive Materials
PATRAM 2019
August 4-9, 2019, New Orleans, LA, USA

Topic: Shielding Material – Production and Analysis

Sintering Behavior of Al-B_4C Powder Material and its Phase Evolution during Rolling

Stefan Pretterhofer[1,2], Herbert Frühwirth[2], Dr. Christian Gierl-Mayer[2], Prof. Herbert Danninger[2]

[1] voestalpine BÖHLER Bleche GmbH & Co KG, 8680 Muerzzuschlag, Austria

[2] Institute of Chemical Technologies and Analytics, TU Wien, 1060 Vienna, Austria

Abstract

Metal matrix composites (MMC) samples consisting of aluminum and boron carbide were prepared through the powder metallurgy route. In a first step, the sintering behavior of the so-produced slab was investigated. Subsequently new samples were hot rolled in a 2-high rolling mill to 1/6 of the initial diameter.

To evaluate microstructure and chemical composition of the emerging phases of the produced composites, optical microscopy (OM), X-ray diffraction analysis (XRD) and scanning electron microscopy (SEM) with energy dispersive X-ray spectroscopy (EDX) were applied. Mechanical properties of the specimens were investigated by tensile tests. To analyze the neutron attenuation behavior JEN-3 test was applied. This tool is a neutron absorption testing equipment that is used in the industry for non-destructive material inspection.

Significant shrinkage does not occur, however, sintering has functioned properly as can be seen by the metallic sintered necks present after the heat treatment.

Furthermore, the density after rolling is 100%. Therefore, it can be stated that the combination of temperature and mechanical deformation leads to a fully dense material. This is also corroborated by the results of the tensile tests. The microstructure of the MMC material shows the B_4C particles properly distributed in the aluminum matrix. Although a diffusion zone can be seen in the EDX analysis, no new phases appear in the material. This is also in accordance with the XRD results. The mentioned diffusion zone is also an indicator for proper interfacial bonding of the two types of powder in the material. In a case, the neutron attenuation behavior is not influenced and is homogeneous within the sheet as well as sufficiently high.

1 Introduction

Metal matrix composites consisting of an aluminum matrix reinforced with B_4C particles have several advanced structural properties such as low density, high strength, especially related to the low density (specific strength), stiffness, erosion and wear resistance [1–4]. One of the main benefits of this material is the good mixture of properties for shielding applications in the nuclear industry [5]. Due to the high natural abundance of ^{10}B in boron element (~19.8 %) [6] with its vast thermal neutron capture cross section (3837 barn) [7], B_4C is suitable for capturing thermal neutrons. In combination with high ductility and superb thermal conductivity of the matrix metal, this material is widely used in the nuclear industry. [5]

In the recent decades, simultaneously with the development of this metal matrix composite, a number of manufacturing techniques, such as stir casting [8], squeeze casting, pressure and pressure-less infiltration [9], spark plasma sintering [10], accumulative roll bonding [11] and powder metallurgy [12] have been developed.

Two powder metallurgy production routes are dominant to manufacture highly reinforced (up to ~35%) Al/B_4C sheets and plates. Pressing, sintering, hot extrusion followed by rolling [13], and hot isostatic pressing and rolling [14], respectively. An unusual manufacturing technique is in use at voestalpine BÖHLER Bleche in Austria to produce MMC sheets and plates. This simplified route consists of axial pressing, sintering and rolling.

We have performed two series of experiments to find the perfect conditions for the production of sheets. Firstly, the aim of this study is the investigation of the sintering behavior of Al-B_4C powder material. Therefore, pressed and sintered specimens were produced. In a second step a thorough analysis of sheet material was performed. For this purpose larger samples were prepared in a way that rolling was feasible. This study comprises tensile testing to evaluate the mechanical properties as well as optical and SEM micrographs to assess the occurring microstructure. Furthermore, X-ray diffraction analysis and energy dispersive X-ray spectrometry to determine the chemical composition were conducted. In this study the neutron attenuation behavior was also evaluated – mainly to prove the homogeneity of the so-produced material.

2 Experiments

Boron carbide and 1070 Al alloy powders were used as starting material. The mean particle sizes were 18,5 µm and 25 µm , respectively. In Table 1 the chemical composition of the B_4C powder is given.

Table 1. Chemical Composition of B_4C (wt./%)

B	C	O	N	Cl	F	Ca	Fe	Si
79.20	20.14	0.10	0.06	<0.0005	<0.0005	0.01	0.09	0.13

2.1 Pressing and Sintering

A tumbling mixer with steel balls was used to blend the 1070 Al alloy and B_4C powders for 10 min at weight ratios 9:1, 8:2 and 7:3, respectively. Ball-to-powder ratio of 1:2 was applied. Firstly, samples of 55 x 10 x 5.5 mm^3 were die-pressed to investigate the consolidation behavior of this material. The sintering process of the so-produced samples took place in a nitrogen atmosphere at elevated temperatures below the melting point of Al.
The sintering behavior of the blended and pressed powder was analyzed using scanning electron microscopy by taking secondary electron images of the fracture surfaces. The metallographic sections were evaluated by optical microscopy.

2.2 Pressing, Encapsulating, Sintering and Rolling

Larger samples are needed to evaluate the mechanical properties of plates of this material. Therefore, the as-mixed powders were compacted in an aluminum capsule (alloy 6061). Four samples of MMC10 (total weight ratio: 9:1) and two samples of MMC30 (total weight ratio: 7:3) sized 120x160x30 mm^3 were produced. Blending was executed in a screw cone type mixer for 30 min at room temperature. The pressed and sintered samples were reheated to forming temperature and rolled to a thickness of 5 mm. Three different rolling schedules were used. A

rough one (sample 15 & 21), a medium one (sample 14 & 20) and a soft one (sample 12 & 18), respectively. Subsequently, annealing was performed.
The microstructure and chemical composition was evaluated by OM and SEM/EDX, respectively. To validate the EDX measurements, XRD study was conducted as well. Standard tensile testing was used to evaluate the mechanical properties of the so-produced material. Additionally, a neutron attenuation behavior test was performed on the MMC30 sample. The so-called JEN-3 method is comprised of a Cf-252 neutron source and a scintillation detector. This neutron absorption equipment is illustrated in Figure 1. For the measurement the sample is placed on a neutron reflective polyethylene desk. The fast neutrons from the source pass through the sheet, are slowed down to thermal neutrons in the reflector and travel back through the sample. The detector measures the reflected thermalized neutrons [5, 15]. Every 50 mm 50 measurements were taken to both study the attenuation behavior in general and to prove the homogeneity of the sheet.

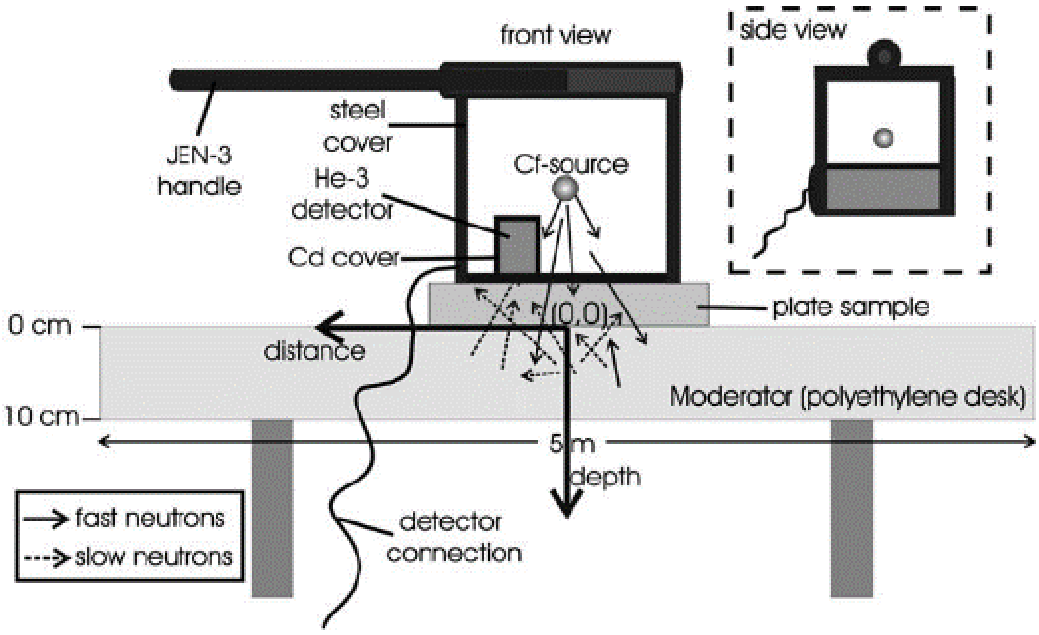

Figure 1. Layout and principle of the JEN-3 neutron attenuation tool [15]

3 Results of the pressed and sintered MMCs

3.1 Sintering behavior

Figure 2 (a) shows an optical micrograph of the pressed and sintered MMC10 material whereas (b) shows a SEM micrograph of the fracture surface thereof. Although some pores can be seen in the OM, sintering has functioned properly as visible from the microstructure. It can be seen that no distinct aluminum particle is visible in the material after the sintering process. Also, the boron carbide particles are distributed uniformly in the metal matrix. In the SEM micrograph boron carbides within a distinctly connected matrix is shown. This also supports the assumption that sintering has functioned properly.

(a) (b)

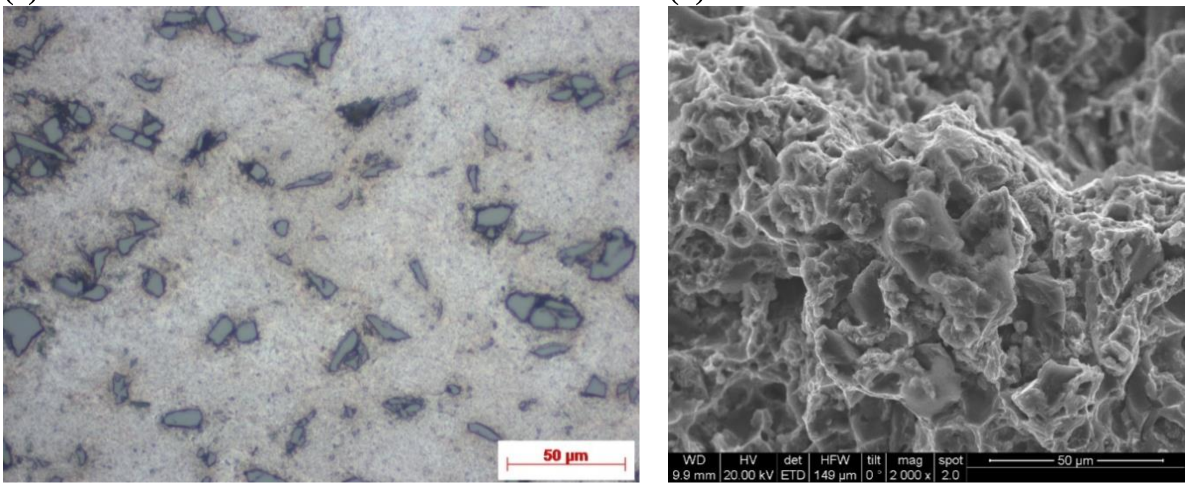

Figure 2. Microstructure recorded via optical microscopy (a) and SEM micrograph of fracture surface (b) of pressed and sintered MMC10

4 Results of the pressed, capsuled, sintered and rolled MMCs

4.1 Microstructure

The microstructure of the final sheets is presented in Figure 3. It can be seen that the B_4C particles are homogeneously distributed in the aluminum matrix. Obviously, the higher the carbide content the more B_4C can be found in the optical micrograph. Although different rolling schedules were applied, the distribution of the particles is not affected thereof. The microstructure also appears to be fully dense.

4.2 Phase Evolution and Chemical Composition

In Figure 4 an elemental mapping of sample 15 (MMC10) is shown. In the electron backscattered micrograph two distinct phases can be seen. Although an aluminum gradient is present in the interface layer between boron carbide and aluminum, which can be seen in the elemental profile plot in Figure 5, no new phase can be detected in this area. The interfacial elemental gradient also indicates well embedded B_4C particles in the metal matrix. Therefore, it can be stated that reinforcement has functioned properly. However, little can be said about the behavior of boron and carbon because of the limited possibilities to measure these light elements with EDX. Nevertheless, Figure 4 shows that elements boron and carbon can only be found in the boron carbide areas. Therefore, it can be concluded that no other phase is formed during the production of the sheet. This is also in accordance with the XRD measurement. In Figure 6 the result of this study is represented. It can be seen that no other phase than the two mentioned are present. Calcite is also listed but does not need to be considered because of its presence in the embedding resin.

4.3 Mechanical Properties

Three tensile tests per sheet were conducted to ascertain the mechanical properties. The results of the said tests is illustrated in Figure 7. It can be seen that for the higher B_4C content, in this case MMC30, both the yield strength and the ultimate tensile strength, are slightly higher. However, compared with the MMC10 samples the total elongation is remarkably lower. Both findings are in accordance with the results from commercially available products [16, 17]. Also, the quantitative results are within the range of the well-known industrial products [16–20].

MMC30 – Sample 12 (soft rolling) – 500x –center

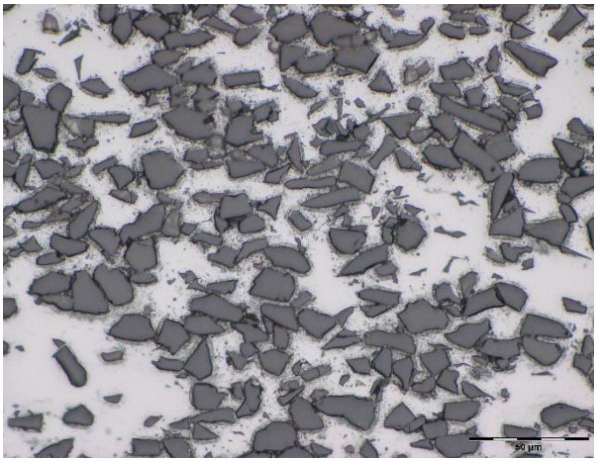

MMC30 – Sample 12 – 100x – interface area

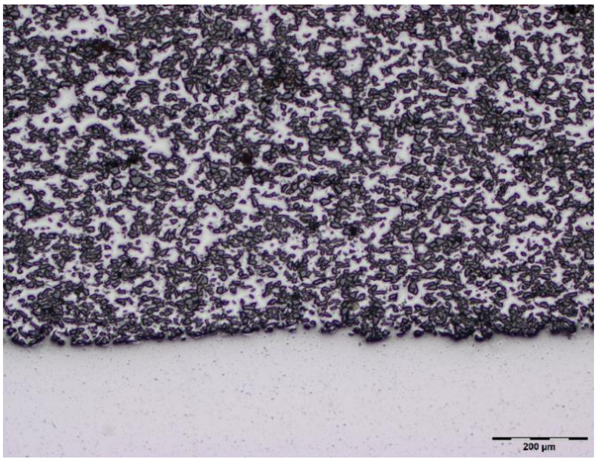

MMC10 – Sample 14 (medium rolling) – 500x – center

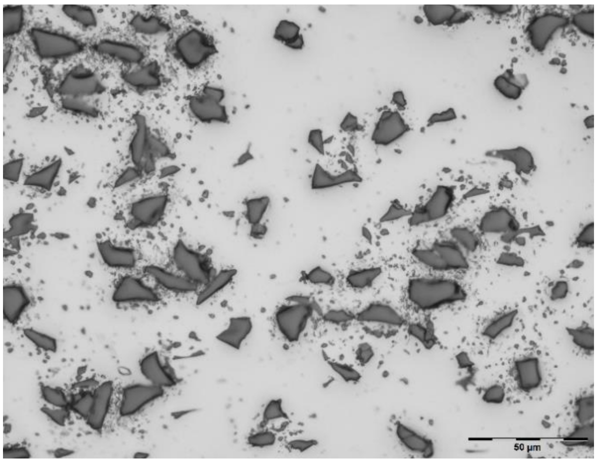

MMC10 – Sample 15 (rough rolling) – 500x – center

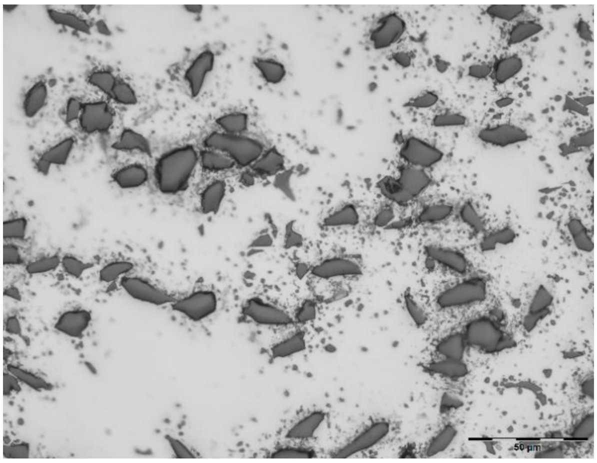

MMC10 – Sample 20 (medium rollng) – 500x – center

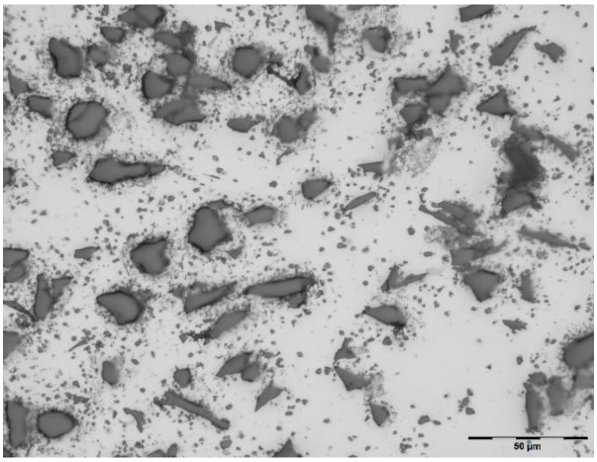

MMC10 – Sample 21 (rough rolling) – 500x – center

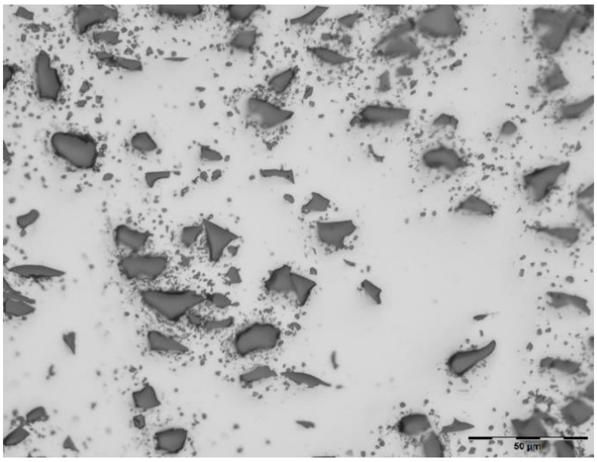

Figure 3. Optical micrographs of rolled B_4C/1070 Al composites with various B_4C contents and various rolling schedules

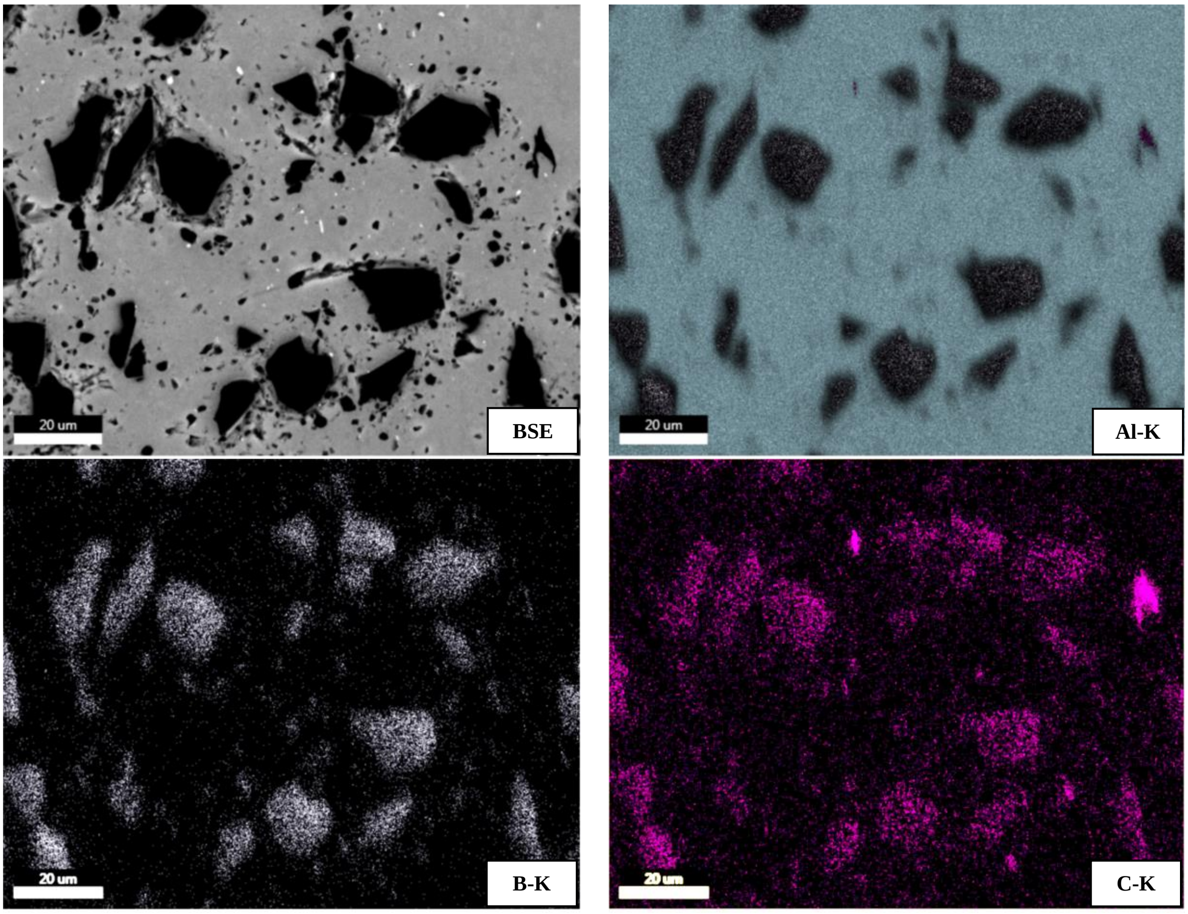

Figure 4. SEM-EDX elemental mapping of sample 15: Backscattered electron microscopy + distribution maps of Al, B and C (Brightness and contrast of B and C mapping had to be adjusted)

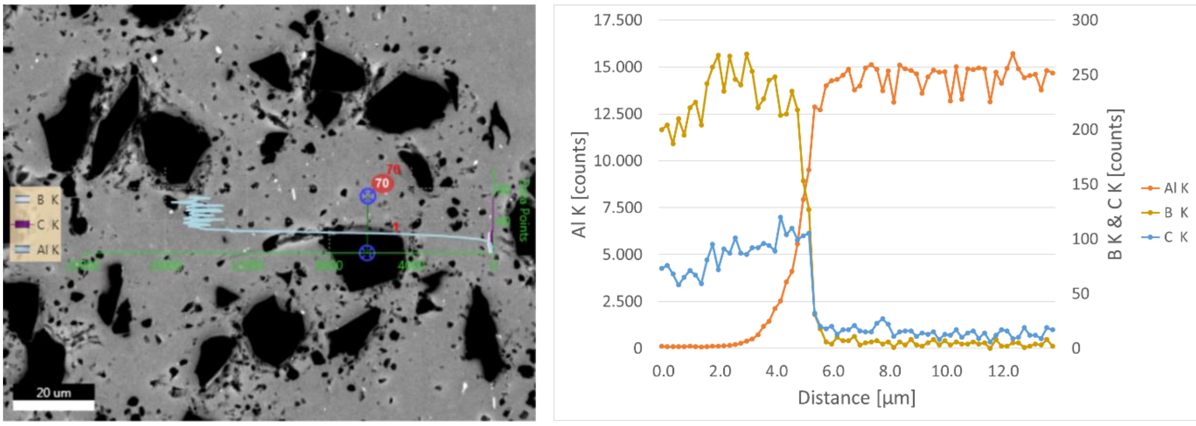

Figure 5. SEM-EDX element profile plot of sample 15

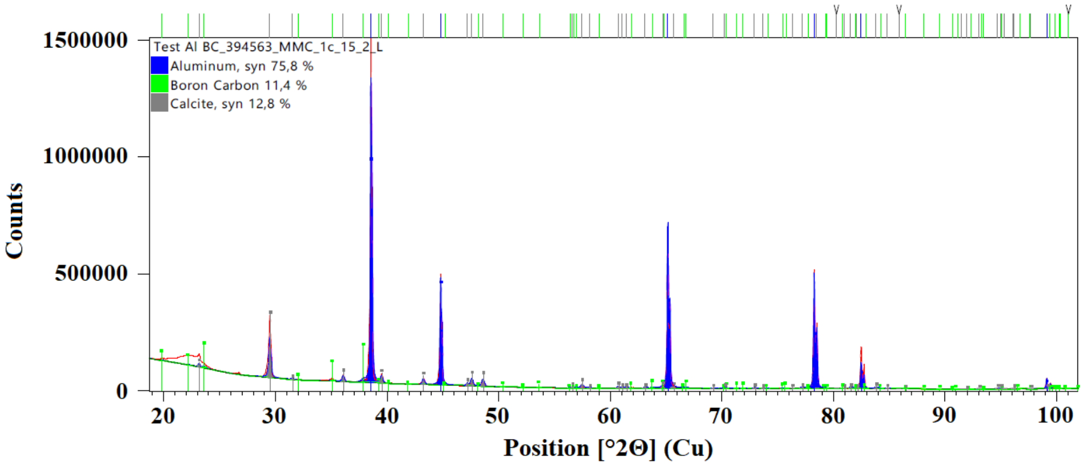

Figure 6. XRD pattern of sample 15

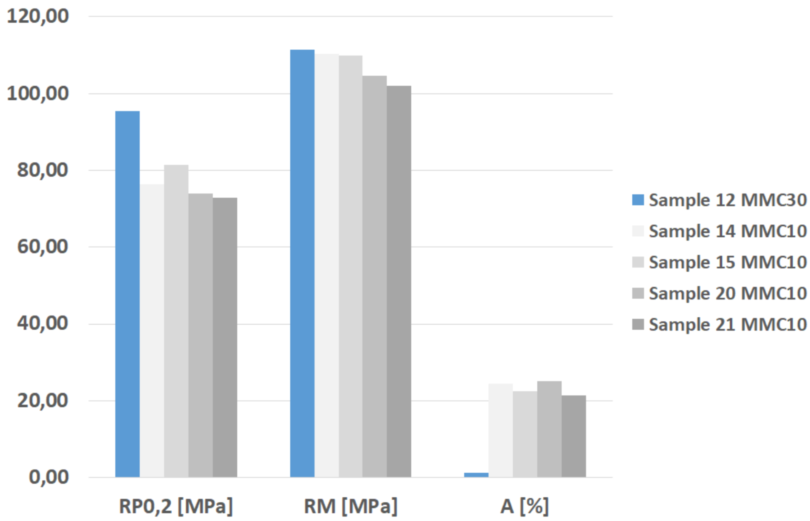

Figure 7. Tensile test results

4.4 Neutron attenuation behavior

Neutron absorption measurements of sample 18 using the JEN-3 tool were conducted as described in chapter 2. Sample 18 consists of 30 wt.% B_4C (MMC30) and is illustrated in Figure 9 together with a schematic map of the measurement positions of the JEN-3 tool. As can be seen in this figure the sheet is too small for measurements. Therefore, two commercially available MMC30 sheets of 5 mm thickness were placed next to the sample. The neutron attenuation measurements of these sheets revealed an average count rate of 35723 and a standard deviation of 143 digits, respectively. Since the absorption in the commercially available sheets is in the range of the tested ones, the results should not be much influenced by the chosen measurement setup. Fifty measurements at every measurement position were taken. In Figure 8, the mean values with the corresponding standard deviations depending on the position on the sheet are illustrated. The neutron attenuation is sufficiently high compared with the commercially available MMC30 sheet. Furthermore, there is no significant variation of the neutron attenuation behavior in sample 18. Since the neutron absorption is directly related to the presence of ^{10}B, this result indicates that B_4C is homogeneously distributed in the material.

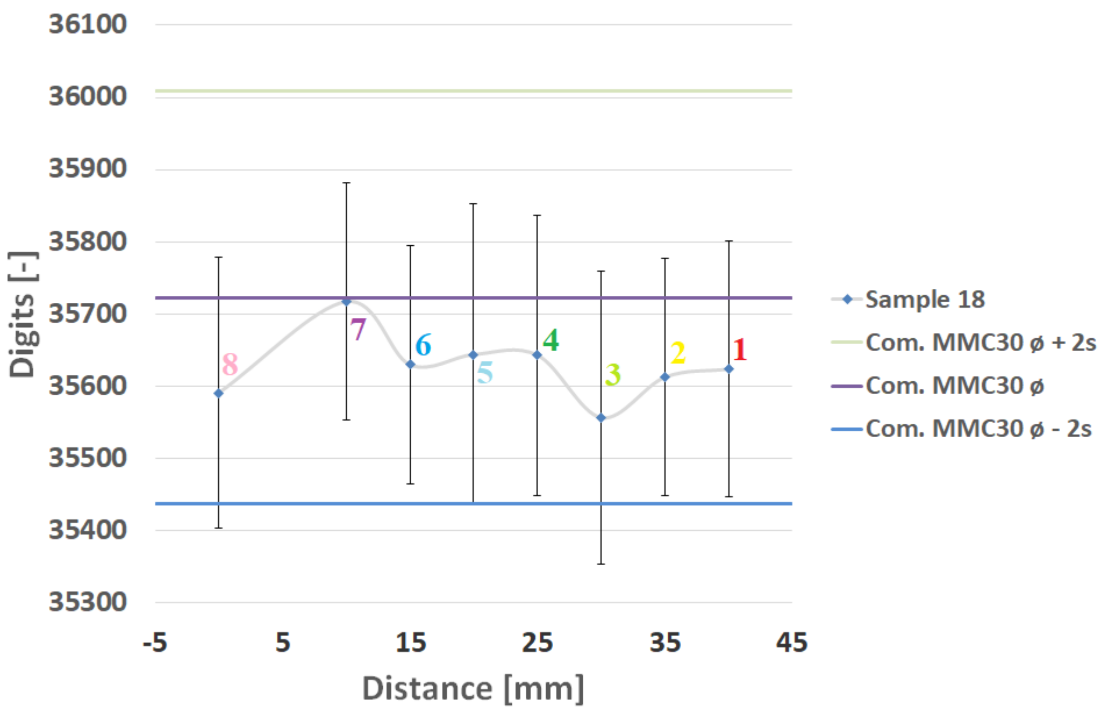

Figure 8. Results of neutron attenuation measurements using JEN-3

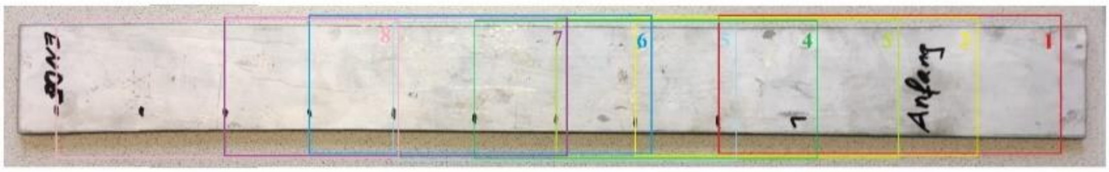

Figure 9. Sample 18 with a schematic map of each measurement position of the JEN-3 neutron attenuation tool

5 Conclusions

5.1 <u>Pressed and sintered MMCs</u>

Appropriate conditions to sinter metal matrix composites consisting of Al and B_4C were found. Furthermore, the microstructure shows a homogeneous distribution. Nevertheless, pores are present in the not-rolled material.

5.2 <u>Pressed, capsuled, sintered and rolled MMCs</u>

Subsequently, MMC sheets were produced. The microstructure reveals a homogeneous distribution of ceramic particles in an aluminum matrix. Neither voids nor pores could be found in the investigated material. Moreover, the mechanical properties of these sheets are within the range of commercially fabricated PM Al-B_4C products. Therefore, it can be concluded that the described production process is sufficient to manufacture fully dense MMC sheets with both usual mechanical properties and uniformly distributed reinforcement. The latter is also confirmed by the neutron attenuation test results. Also the shielding properties are comparable with commercially available products in this sector. In addition, the phase evolution during the mentioned production method was analyzed. The results of the XRD testing are in accordance with the results of the EDX investigation. Although an Al diffusion zone was detected around the B_4C particles, no new distinctive phase could be found in this area. In addition, the XRD measurement indicates only the two mixed phases, Al and boron carbide, respectively. The bottom line of this survey is, although bonding of the ceramic particles with the metal matrix has functioned properly, no new phases occurred applying the powder metallurgy production route.

6 References

1. Bonnet G, Rohr V, Chen X-G et al. (2009) Use of Alcan's Al-B 4 C metal matrix composites as neutron absorber material in TN International's transportation and storage casks. Packaging, Transport, Storage & Security of Radioactive Material 20(3): 98–102. doi: 10.1179/174651009X416880

2. Topcu I, Gulsoy HO, Kadioglu N et al. (2009) Processing and mechanical properties of B4C reinforced Al matrix composites. Journal of Alloys and Compounds 482(1): 516–521. doi: 10.1016/j.jallcom.2009.04.065

3. A. R. Kennedy (2002) The microstructure and mechanical properties of Al-Si-B4C metal matrix composites. Journal of Materials Science(37): 317–323

4. Previtali B, Pocci D, Taccardo C (2008) Application of traditional investment casting process to aluminium matrix composites. Composites Part A: Applied Science and Manufacturing 39(10): 1606–1617. doi: 10.1016/j.compositesa.2008.07.001

5. EPRI (2009) Handbook of Neutron Absorber Materials for Spent Nuclear Fuel Transportation and Storage Applications: 2009 Edition. https://www.epri.com/#/pages/product/1019110/?lang=en-US. Accessed 23 May 2019

6. Huang Y, Liang L, Xu J et al. (2012) The design study of a new nuclear protection material. Nuclear Engineering and Design 248: 22–27. doi: 10.1016/j.nucengdes.2012.03.016

7. C.Subramanian, A.K.Suri, T.S.R.Ch.Murthy (2010) Development of Boron-based materials for nuclear applications. BARC Newsletter(313): 14–22

8. Shorowordi KM, Laoui T, Haseeb ASMA et al. (2003) Microstructure and interface characteristics of B4C, SiC and Al2O3 reinforced Al matrix composites: a comparative study. Journal of Materials Processing Technology 142(3): 738–743. doi: 10.1016/S0924-0136(03)00815-X

9. Clyne TW, Withers PJ (2010) Introduction to Metal Matrix Composites. Cambridge Solid State Science. Cambridge University Press, Cambridge, GBR

10. Vintila R, Charest A, Drew RAL et al. (2011) Synthesis and consolidation via spark plasma sintering of nanostructured Al-5356/B4C composite. Materials Science and Engineering: A 528(13-14): 4395–4407. doi: 10.1016/j.msea.2011.02.079

11. Alizadeh M, beni HA, Ghaffari M et al. (2013) Properties of high specific strength Al–4wt.% Al2O3/B4C nano-composite produced by accumulative roll bonding process. Materials & Design 50: 427–432. doi: 10.1016/j.matdes.2013.03.018

12. Everett RK, Arsenault RJ (1991) Metal matrix composites: Processing and Interfaces. Treatise on materials science and technology. Academic Press, Boston

13. Chen HS, Wang WX, Nie HH et al. (2018) Microstructure evolution and mechanical properties of B4C/6061Al neutron absorber composite sheets fabricated by powder

metallurgy. Journal of Alloys and Compounds 730: 342–351. doi: 10.1016/j.jallcom.2017.09.312

14. Zhang H, Ramesh KT, Chin ESC (2004) High strain rate response of aluminum 6092/B4C composites. Materials Science and Engineering: A 384(1-2): 26–34. doi: 10.1016/j.msea.2004.05.027

15. Bastürk M, Arztmann J, Jerlich W et al. (2005) Analysis of neutron attenuation in boron-alloyed stainless steek with neutron radiography and JEN-3 gauge. Journal of Nuclear Materials 341(2-3): 189–200. doi: 10.1016/j.jnucmat.2005.02.003

16. Ceradyne Canada (2013) Neutron Absorber Materials for Fresh and Spent Fuel Applications: Slide Presentation from 3/14/13 Public Meeting on Neutron Absorbing Materials. https://www.nrc.gov/docs/ML1307/ML13079A557.pdf. Accessed 23 May 2019

17. EPRI (2001) Qualification of METAMIC® for Spent-Fuel Storage Application. https://www.epri.com/#/pages/product/1003137/?lang=en-US. Accessed 23 May 2019

18. United States Nuclear Regulatory Commission (2008) Material Qualification of Alcan Composite for Spent Fuel Storage. https://www.nrc.gov/docs/ML1319/ML13199A039.pdf. Accessed 22 May 2019

19. Northeast Technology Corp. (2003) BORTEC Qualification Program For Nuclear Fuel Storage Applications. http://www.dwatechnologies.com/documents/NET-205-02%20Final%20Test%20Results%20Rev%201.pdf. Accessed 22 May 2019

20. dwa Technologies I Bortec Neutron Absorbing Sheets. http://dwatechnologies.com/documents/DWA_BORTEC_Sheets_v05.pdf. Accessed 23 May 2019